1521-0111/88/2/265–272$25.00
MOLECULAR PHARMACOLOGY

http://dx.doi.org/10.1124/mol.115.099333
Mol Pharmacol 88:265–272, August 2015

The Lysophosphatidylinositol Receptor GPR55 Modulates Pain Perception in the Periaqueductal Gray

Elena Deliu, Margaret Sperow, Linda Console-Bram, Rhonda L. Carter, Douglas G. Tilley, Daniel J. Kalamarides, Lynn G. Kirby, G. Cristina Brailoiu, Eugen Brailoiu, Khalid Benamar,[1] and Mary E. Abood

Center for Substance Abuse Research (E.D., M.S., L.C.-B., D.J.K., L.G.K., E.B., K.B., M.E.A.), Department of Anatomy and Cell Biology (L.G.K., M.E.A.), Center for Translational Medicine and Department of Pharmacology (R.L.C., D.G.T.), Temple University School of Medicine, Philadelphia, Pennslyvania; and Department of Pharmaceutical Sciences, Thomas Jefferson University School of Pharmacy, Philadelphia, Pennsylvania (G.C.B.)

Received April 6, 2015; accepted May 12, 2015

ABSTRACT

Emerging evidence indicates the involvement of GPR55 and its proposed endogenous ligand, lysophosphatidylinositol (LPI), in nociception, yet their role in central pain processing has not been explored. Using Ca^{2+} imaging, we show here that LPI elicits concentration-dependent and GPR55-mediated increases in intracellular Ca^{2+} levels in dissociated rat periaqueductal gray (PAG) neurons, which express GPR55 mRNA. This effect is mediated by Ca^{2+} release from the endoplasmic reticulum via inositol 1,4,5-trisphosphate receptors and by Ca^{2+} entry via P/Q-type of voltage-gated Ca^{2+} channels. Moreover, LPI depolarizes PAG neurons and upon intra-PAG microinjection, reduces nociceptive threshold in the hot-plate test. Both these effects are dependent on GPR55 activation, because they are abolished by pretreatment with ML-193 [*N*-(4-(*N*-(3,4-dimethylisoxazol-5-yl)sulfamoyl)-phenyl)-6,8-dimethyl-2-(pyridin-2-yl)quinoline-4-carboxamide], a selective GPR55 antagonist. Thus, we provide the first pharmacological evidence that GPR55 activation at central levels is pronociceptive, suggesting that interfering with GPR55 signaling in the PAG may promote analgesia.

Introduction

GPR55 is a lysophosphatidylinositol (LPI)-sensitive receptor that has also been involved in cannabinoid signaling (Henstridge, 2012). Both GPR55 and LPI may play a role in pain modulation. GPR55 null mice do not develop mechanical hyperalgesia post-intraplantar injection of Freund's complete adjuvant nor after partial nerve ligation, suggesting a putative therapeutic potential of GPR55 manipulation in inflammatory and neuropathic pain (Staton et al., 2008). Loss of GPR55 also results in a mild perturbation of thermal nociception in the hot-plate test (Staton et al., 2008) and has been associated with a significant reduction in cancer-associated pain (Staton et al., 2008; Wu et al., 2013). LPI-induced stimulation of sensory afferents has recently been correlated with dose-dependent development of mechanical hypersensitivity, allodynia, and hyperalgesia, which were partially mediated by GPR55 (Gangadharan et al., 2013).

LPI, which endogenously activates GPR55, is intracellularly generated by the Ca^{2+}-dependent cytosolic phospholipase A2, cPLA2 (Pineiro and Falasca, 2012). Central cPLA2 inhibition via intracerebroventricular injection of selective blockers results in reduced pain perception in mice undergoing facial carrageenan injection (Yeo et al., 2004). Moreover, LPI levels are increased in the caudal medulla oblongata of carrageenan-injected rats (Ma et al., 2012). Although GPR55 is widely expressed throughout the central nervous system (Henstridge et al., 2011), a role for GPR55 in pain modulation at central levels has not been explored.

The periaqueductal gray (PAG) is a critical site where nociceptive transmission is modulated. Via projections through the rostral ventromedial medulla, the PAG sends either pain-inhibiting or pain-facilitating outputs to dorsal horn laminae involved in nociceptive function (Heinricher et al., 2009). Typically, inflammation and nerve injury, in which GPR55 has been shown to play a pronociceptive role (Staton et al., 2008), are correlated with PAG-mediated descending facilitation, hyperalgesia, and chronic pain (Porreca et al., 2002; Heinricher et al., 2009). To investigate whether GPR55 modulates nociceptive transmission in the periaqueductal gray, we examined the effects of GPR55 activation and blockade on PAG neurons in vitro and in vivo.

This work was supported by the National Institutes of Health National Institute of Drug Abuse [Grants R01-DA035926, T32-DA007237, P30-DA013429, R01-HL105414]. The authors declare no competing financial interests.

[1]Current affiliation: Department of Pharmacology and Neuroscience, Texas Tech University Health Sciences Center, School of Medicine, Lubbock, Texas.

dx.doi.org/10.1124/mol.115.099333.

ABBREVIATIONS: aCSF, artificial cerebrospinal fluid; $DiBAC_4(3)$, bis-(1,3-dibutylbarbituric acid) trimethine oxonol; HBSS, Hank's balanced salt solution; IP_3R, inositol 1,4,5-trisphoshate receptor; LPI, lysophosphatidylinositol; ML-193, *N*-(4-(*N*-(3,4-dimethylisoxazol-5-yl)sulfamoyl)-phenyl)-6,8-dimethyl-2-(pyridin-2-yl)quinoline-4-carboxamide; PAG, periaqueductal gray; VGCC, voltage-gated Ca^{2+} channels.

Materials and Methods

Chemicals. Soy LPI was obtained from Avanti Polar Lipids (Alabaster, AL). ML-193 (CID 1261822), *N*-(4-(*N*-(3,4-dimethylisoxazol-5-yl)sulfamoyl)-phenyl)-6,8-dimethyl-2-(pyridin-2-yl)quinoline-4-carboxamide, was obtained from MolPort (Riga, Latvia). *trans*-Ned-19 was obtained from Tocris Biosciences (R&D Systems, Minneapolis, MN); ryanodine and xestospongin C were from EMD Millipore (Billerica, MA). 2-Aminoethoxydiphenil borate, ω-conotoxin MVIIC, ω-conotoxin GVIA, and nifedipine were from Sigma-Aldrich (St. Louis, MO). All other chemicals were obtained from standard laboratory chemical suppliers.

Animals. Neonatal Sprague-Dawley rats (1–2 days old) (Charles River Laboratories, Wilmington, MA) of either sex were used for neuronal culture. Male juvenile Sprague-Dawley rats (4–5 weeks old) (Taconic Farms, Germantown, NY) were used for in vitro electrophysiology studies. For in vivo studies, male Sprague-Dawley rats (Ace Animals, Boyertown, PA), weighing 175–200 g, were housed in groups of 2–3 for at least 1 week in an animal room maintained at 22 ± 1°C and approximately 50 ± 2% relative humidity. Lighting was on a 12/12-hour light/dark cycle (lights on at 07:00 and off at 19:00). The animals were allowed free access to food and water.

All animal use procedures were conducted in strict accordance with the National Institutes of Health Guide for the Care and Use of Laboratory Animals and were approved by Temple University Institutional Animal Care and Use Committee.

Cells. U2OS cells permanently expressing HA-GPR55E and βarr2-GFP (green fluorescent protein) (hitherto GPR55-U2OS) were obtained from Drs. Larry Barak and Marc Caron (Duke University) and have previously been described (Kapur et al., 2009). GPR55-U2OS and control, untransfected U2OS cells were maintained in Dulbecco's modified Eagle's medium (Cellgro, Mediatech, Herndon, VA) supplemented with 10% fetal bovine serum (Mediatech), 50 μg/ml Zeocin (Invitrogen, Carlsbad, CA), and 100 μg/ml G418 (A.G. Scientific, San Diego, CA) at 37°C in a humidified incubator with 5% CO_2.

PAG neurons were dissociated from neonatal (1–2 day old) Sprague Dawley rats (Charles River Laboratories) of both sexes as previously described (Brailoiu et al., 2012; Deliu et al., 2014). Newborn rats were decapitated and the brains quickly removed surgically and immersed in ice-cold Hanks balanced salt solution (HBSS) (Mediatech).The PAG was identified (Paxinos and Watson, 1988), removed, minced, and subjected to enzymatic digestion (papain, 5 minutes, 37°C), followed by mechanical trituration in presence of total medium—Neurobasal A (Invitrogen) containing 1% GlutaMax (Invitrogen), 2% penicillin-streptomycin-amphotericin B solution (Mediatech), and 10% fetal bovine serum. Cells were cultured on round 25 mm glass coverslips coated with poly-L-lysine (Sigma-Aldrich) in six-well plates. Cultures were maintained at 37°C in a humidified atmosphere with 5% CO_2. The mitotic inhibitor cytosine β-arabinofuranoside (1 μM) (Sigma-Aldrich) was added to the culture the third day to inhibit glial cell proliferation. Cells were imaged after 3–5 days in culture.

Real-Time Reverse Transcription Polymerase Chain Reaction. Total RNA was isolated from isolated rat brain cortex PAG using an RNeasy Midi kit or RNeasy Fibrous Tissue Midi kit with Proteinase K and DNAseI digestion (Qiagen, Valencia, CA), cDNA was synthesized using a High Capacity cDNA Reverse Transcription kit (Applied Biosystems, Foster City, CA), and real-time polymerase chain reaction was performed with TaqMan Gene Expression Master Mix (Applied Biosystems) using the StepOne Plus Realtime PCR System (Applied Biosystems). Primer sets used were: Rn03037213-second1 (GPR55) and Rn01775763-g1 (GAPDH, for normalization) and were attained from Applied Biosystems. All samples were run in triplicate, and data were analyzed using Applied Biosystems Comparative CT Method (ΔΔCT).

Calcium Imaging. The intracellular Ca^{2+} concentration, $[Ca^{2+}]_i$, was measured as previously described (Brailoiu et al., 2012; Deliu et al., 2014). Cells were incubated with 5 μM fura-2 AM (Invitrogen) in HBSS at room temperature for 45 minutes in the dark, washed three times with dye-free HBSS, and then incubated for another 45 minutes to allow for complete de-esterification of the dye. Coverslips (25 mm diameter) were subsequently mounted in an open bath chamber (RP-40LP; Warner Instruments, Hamden, CT) on the stage of an inverted microscope Nikon Eclipse TiE (Nikon Inc., Melville, NY). The microscope is equipped with a Perfect Focus System and a Photometrics CoolSnap HQ2 charge-coupled device camera (Photometrics, Tucson, AZ). During the experiments, the Perfect Focus System was activated. Fura-2 AM fluorescence (emission = 510 nm), after alternate excitation at 340 and 380 nm, was acquired at a frequency of 0.25 Hz. Images were acquired and analyzed using NIS-Elements AR 3.1 software (Nikon Inc.). After appropriate calibration with ionomycin (EMD Millipore) and $CaCl_2$ and Ca^{2+} free and EGTA, respectively, the ratio of the fluorescence signals (340/380 nm) was converted to Ca^{2+} concentrations. In Ca^{2+}-free experiments, $CaCl_2$ was omitted.

Measurement of Membrane Potential. The relative changes in membrane potential of single neurons were evaluated using bis-(1,3-dibutylbarbituric acid) trimethine oxonol, $DiBAC_4(3)$ (Invitrogen), a slow response voltage-sensitive dye, as previously described (Yu et al., 2013; Deliu et al., 2014). Upon membrane hyperpolarization, the dye concentrates in the cell membrane, leading to a decrease in fluorescence intensity, whereas depolarization induces the sequestration of the dye into the cytosol, resulting in an increase of the fluorescence intensity. Cultured PAG neurons were incubated for 30 minutes in HBSS containing 0.5 mM $DiBAC_4(3)$, and the fluorescence was monitored at 0.17 Hz, excitation/emission: 480/540 nm. Calibration of $DiBAC_4(3)$ fluorescence after background subtraction was performed using the Na^+-K^+ ionophore gramicidin in Na^+-free physiologic solution and various concentrations of K^+ (to alter membrane potential) and *N*-methylglucamine (to maintain osmolarity). Under these conditions, the membrane potential was approximately equal to the K^+ equilibrium potential determined by the Nernst equation. The intracellular K^+ and Na^+ concentration were assumed to be 130 and 10 mM, respectively.

Electrophysiology. Visualized whole cell patch clamp was performed on midbrain slices from 4- to 5-week-old rats, as previously described (Heinisch and Kirby, 2010; Chen et al., 2011; Deliu et al., 2012). Rats were rapidly decapitated and the head placed in ice-cold artificial cerebrospinal fluid (aCSF) in which sucrose (248 mM) was substituted for NaCl. The brain was quickly removed and trimmed to isolate the brain stem region. Slices 300 μm thick were cut throughout the rostrocaudal extent of the PAG using a Vibratome 3000 Plus (Vibratome, St. Louis, MO) and placed in a holding vial containing aCSF at 35°C bubbled with 95% O_2/5% CO_2 for 1 hour. Slices were then maintained in room temperature aCSF bubbled with 95% O_2/5% CO_2. The composition of the aCSF was (in millimolar): NaCl 124, KCl 2.5, NaH_2PO_4 2, $CaCl_2$ 2.5, $MgSO_4$ 2, dextrose 10, and $NaHCO_3$ 26. Slices were transferred to a recording chamber (Warner Instruments) and continuously perfused with aCSF at 1.5–2.0 ml/min at 32–34°C maintained by an in-line solution heater (TC-324; Warner Instruments). Neurons were visualized using a Nikon E600 upright microscope fitted with a 40× water-immersion objective, differential interference contrast, and infrared filter (Optical Apparatus, Ardmore, PA). The image from the microscope was enhanced using a charge-coupled device camera and displayed on a computer monitor. Whole cell recording pipettes were fashioned on a P-97 micropipette puller (Sutter Instruments, Novato, CA) using borosilicate glass capillary tubing (1.2 mm outer diameter, 0.69 mm inner diameter; Warner Instruments). The resistance of the electrodes was 4–8 MΩ when filled with an intracellular solution of (in millimolar) potassium gluconate 130, NaCl 5, $MgCl_2$ 1, EGTA 0.02, HEPES 10, sodium phosphocreatinine 10, MgATP 2, Na_2GTP 0.5, and 0.1% Biocytin, pH 7.3. Recordings were conducted in cells located in the lateral and ventrolateral subdivisions of the PAG at the mid-caudal levels (corresponding to −5.88 mm to −6.84 caudal to bregma in Paxinos and Watson (1988). A visualized cell was approached with the electrode, a gigaohm seal established, and the cell membrane was ruptured to obtain a whole cell recording using a HEKA patch clamp

EPC-10 amplifier (HEKA Elecktronik, Pfalz, Germany). Series resistance was monitored throughout the experiment. If the series resistance was unstable or exceeded four times the electrode resistance, the cell was discarded.

Once the whole cell recording was obtained, cell membrane potential and input resistance were monitored in current-clamp mode (I = 0 pA). Baseline membrane potential was initially recorded for 5 minutes to ensure that the cell was stable. LPI (10–20 μM) was then added to the perfusion bath and recorded for 10 minutes or until a drug effect on the resting membrane potential was observed. If a drug effect was observed, drugs were removed when the response reached steady state for a postdrug washout period. Input resistance was calculated from voltage responses to periodic −300 pA current pulses. Input resistance was calculated based on the average of three voltage responses at baseline or when the drug effect had reached steady state.

Surgical Procedures. Rats were anesthetized with a mixture of ketamine hydrochloride (100–150 mg/kg) and acepromazine maleate (0.2 mg/kg) given intraperitoneally. A sterilized stainless steel C313G guide cannula (22 gauge; Plastics One, Roanoke, VA) was implanted into the PAG. The stereotaxic coordinates were as follows: 7.8 mm posterior to bregma, 0.5 mm from midline, and 5 mm ventral to the dura mater (Paxinos and Watson, 1988). The animals were housed individually after surgery.

Nociceptive Test. A 52°C hot plate (Ugo Basile, Varese, Italy) was used. The baseline response latency was obtained for each animal after two conditioning runs. Each rat was retested on the hot plate at 15 minutes and thereafter at 15-minute intervals up to 60 minutes by using either jumping or hindpaw licking as the nociceptive endpoint, whereas 30 seconds was taken as the cutoff point to avoid tissue damage.

Injections. After a 7-day recovery period, rats were allowed to habituate to test chambers for 1 hour before testing. A volume of 0.5 μl of drug or vehicle was delivered over 1 minute (manually), and the internal cannula was left in place an additional 90 second to allow diffusion. Immediately thereafter, a dummy cannula (C313DC) was inserted into the cannula guide to prevent any contamination.

Histologic Analysis. At the conclusion of experiments, each rat was checked for the correct site of the injection according to our standard histologic procedures (Benamar et al., 2008a,b). Only data from animals in which the site of injection was clearly located within the PAG regions were included in the studies.

Statistical Analysis. All data are reported as means ± S.E.M. and were compared across treatments and time points and analyzed by repeated-measures analysis of variance, followed by Bonferroni's test; paired or unpaired t tests were used in analyzing data from electrophysiological recordings. The data were analyzed by Prism (GraphPad, San Diego, CA) and by Origin 7 (OriginLab Corporation, Northampton, MA). Significance was set at $P < 0.05$.

Results

LPI Increases Intracellular Ca^{2+} Levels of PAG Neurons via GPR55 Activation. In cultured PAG neurons, LPI (10 μM) administration induced a fast increase in $[Ca^{2+}]_i$, which returned gradually to basal levels (Fig. 1A). In neurons pretreated with GPR55 antagonist ML-193 (10 μM, 20 minutes) (Heynen-Genel et al., 2010), LPI (10 μM) had no effect (Fig. 1A). PAG neurons responded to increasing concentrations of LPI (0.1, 1, and 10 μM) with dose-dependent $[Ca^{2+}]_i$ elevations of 14 ± 2.6 nM (n = 26 cells), 107 ± 3.8 nM (n = 34), and 326 ± 3.4 nM (n = 37), respectively; statistical significance was achieved for the latter two concentrations of LPI ($P < 0.00001$; Fig. 1B). The effect of LPI (10 μM) in PAG neurons pretreated with ML-193 (10 μM, 20 minutes) was negligible ($\Delta[Ca^{2+}]_i$ = 23 ± 3.7 nM, n = 49; Fig. 1B). Representative examples of changes in Fura-2 AM 340/380 fluorescence ratio in cultured PAG neurons in response to LPI in the absence and presence of GPR55 blocker ML-193 are shown in Fig. 1C. We confirmed GPR55 mRNA presence in PAG neurons by quantitative real-time polymerase chain reaction (Fig. 1D).

To assess the activity of GPR55 in cultured PAG neurons, we made use of GPR55-selective pharmacological tools. Although the endogenous GPR55 agonist LPI may promote GPR55-independent Ca^{2+} responses in other paradigms, its GPR55 specificity in the present study was confirmed by the ability of ML-193 to completely block its effect (Fig. 1). We identified ML-193 as a GPR55 selective antagonist in a β-arrestin, high-throughput, high-content screening of 300,000 compounds (Heynen-Genel et al., 2010) and

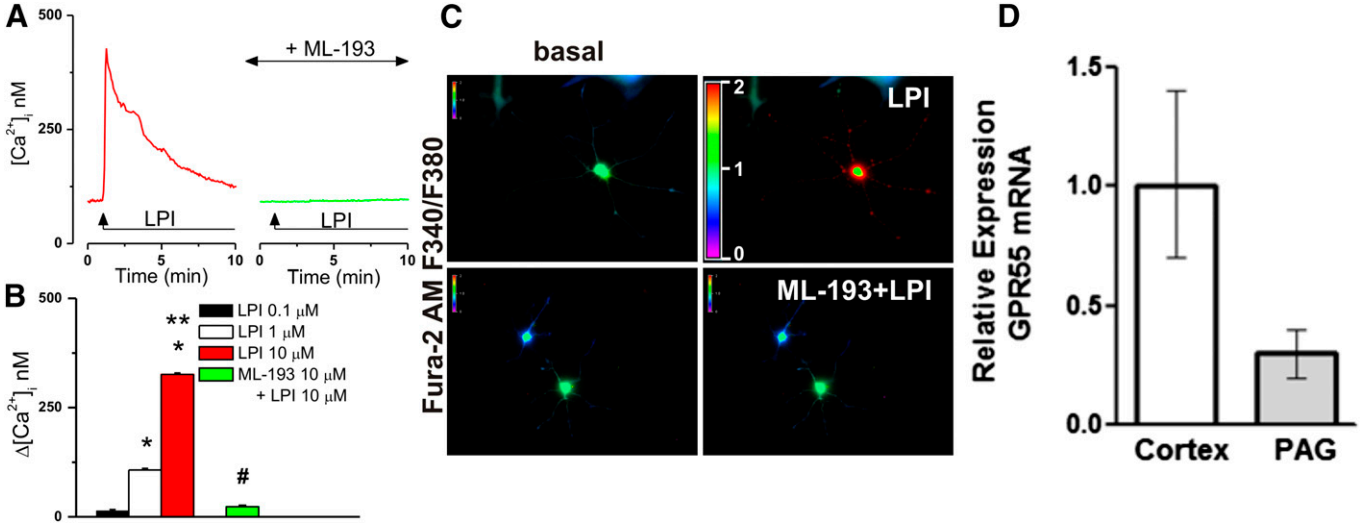

Fig. 1. LPI elicits GPR55-mediated $[Ca^{2+}]_i$ elevation of PAG neurons. (A) Typical tracings of the Ca^{2+} responses elicited by LPI (10 μM) in PAG neurons in the absence and in the presence of GPR55 antagonist ML-193 (10 μM). (B) $[Ca^{2+}]_i$ elevations induced by LPI (0.1, 1, and 10 μM) alone and by LPI (10 μM) in the presence of ML-193 (10 μM); $P < 0.00001$ compared with basal (*), to any other concentration of LPI (**), or to 10 μM LPI (#). (C) Representative images indicating changes in Fura-2 AM fluorescence ratio (340/380 nm) of PAG neurons before and after LPI (10 μM) administration, in absence and presence of ML-193 (10 μM); hot colors indicate significant increases in $[Ca^{2+}]_i$. (D) Relative expression ($\log_{10}$) of GPR55 mRNA in rat brain cortex (tissue with a known high level of GPR55) and PAG.

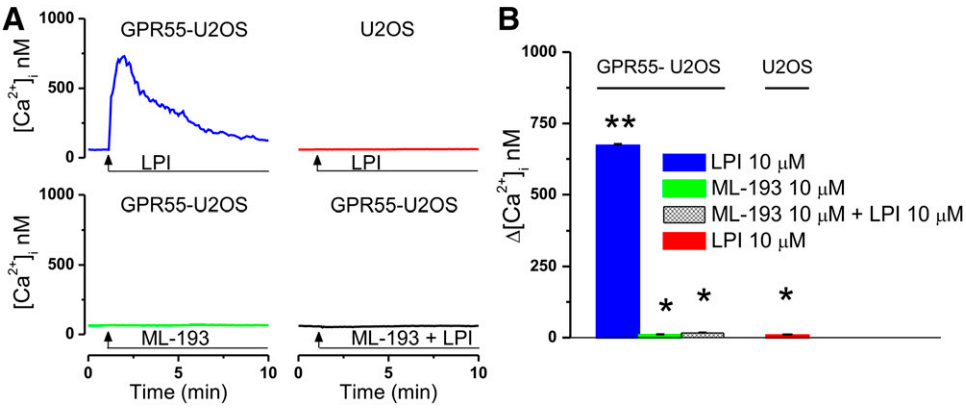

Fig. 2. GPR55 mediates the effects of LPI and ML-193. (A) Representative recordings of the Ca^{2+} responses elicited by LPI (10 μM), ML-193 (10 μM), and by LPI in presence of ML-193 (both 10 μM) in GPR55-U2OS cells and by LPI (10 μM) in untransfected U2OS. (B) Comparison of the responses elicited by treatments indicated in A; $P < 0.05$ compared with basal (**) or to LPI effect in GPR55-U2OS (*).

previously showed that at the concentration tested in the present study, ML-193 lacks any activity at L-type Ca^{2+} channels, inositol 1,4,5-trisphosphate receptors (IP_3Rs), ryanodine receptors, and two-pore channels, whereas it completely antagonizes LPI-mediated Ca^{2+} responses (Yu et al., 2013). To further support the appropriateness of our tools, we evaluated the Ca^{2+} responses of GPR55-U2OS cells and untransfected U2OS cells to LPI and ML-193. As shown in Fig. 2, LPI (10 μM) robustly and significantly elevated $[Ca^{2+}]_i$ in GPR55-U2OS by 672 ± 5.4 nM ($n = 6$ cells) but was largely ineffective in control U2OS cells (8 ± 2.8 nM, $n = 6$; Fig. 2, A and B). Moreover, in GPR55-U2OS cells pretreated with ML-193 (10 μM), the Ca^{2+} response to LPI was basically abolished (16 ± 1.4 nM, $n = 6$), and ML-193 by itself was devoid of an effect (9 ± 2.7 nM, $n = 6$; Fig. 2, A and B).

LPI Produces IP_3R-Mediated Ca^{2+} Release in PAG Neurons. PAG neurons incubated with Ca^{2+}-free saline responded to LPI (10 μM) administration with a rapid and transient elevation in $[Ca^{2+}]_i$, measuring 197 ± 3.4 nM (Fig. 3, A and B). Pretreatment of neurons with Ned-19 (5 μM, 15 minutes), which blocks endolysosomal Ca^{2+} release via nicotinic acid adenine dinucleotide phosphate-sensitive two-pore channels (Naylor et al., 2009) or with ryanodine receptor blocker ryanodine (10 μM, 1 hour), did not significantly modify the Ca^{2+} response to LPI, which measured 184 ± 4.1 nM ($n = 32$) and 192 ± 3.1 nM ($n = 29$), respectively (Fig. 3, A and B). Conversely, blocking IP_3R-mediated Ca^{2+} release with xestospongin C (10 μM, 15 minutes) (Gafni et al., 1997) and 2-aminoethoxydiphenil borate (100 μM, 15 minutes) (Maruyama et al., 1997; Bilmen and Michelangeli, 2002) largely abolished the effect of LPI (10 μM) in Ca^{2+}-free saline ($\Delta[Ca^{2+}]_i = 21 \pm 2.6$ nM, $n = 38$; Fig. 3, A and B).

LPI Promotes Ca^{2+} Influx via P/Q-type of Ca^{2+} Channels. The significant reduction in the amplitude and shape of the LPI-induced Ca^{2+} response observed upon incubation of PAG neurons with Ca^{2+}-free saline (from 326 ± 3.4 to 197 ± 3.4 nM; Fig. 3, A and B) indicated that LPI mobilized both extracellular and intracellular Ca^{2+} pools. Having characterized the latter (Fig. 3), we next examined whether Ca^{2+} influx via voltage-gated Ca^{2+} channels (VGCC) played any role. The effect of LPI was not affected by blocking N-type or L-type of VGCC with ω-conotoxin GVIA (100 nM, 10 minutes; $\Delta[Ca^{2+}]_i = 306 \pm 4.1$ nM, $n = 29$ cells) and nifedipine (1 μM, 10 minutes; $\Delta[Ca^{2+}]_i = 318 \pm 3.9$ nM, $n = 26$), respectively (Fig. 4, A and B); the effect of LPI was fast in onset and returned slowly to baseline in both the absence (Fig. 1A) and in the presence of N-type or L-type VGCC blockers (Fig. 4A). However, in neurons pretreated with ω-conotoxin MVIIC (100 nM, 10 minutes), which inhibits P/Q-type of VGCC, the Ca^{2+} response to LPI was transient and significantly diminished in amplitude ($\Delta[Ca^{2+}]_i = 214 \pm 3.7$ nM, $n = 43$; Fig. 4, A and B).

LPI Induces GPR55-Dependent Depolarization of PAG Neurons. The mean resting membrane potential of PAG neurons was –51.3 ± 0.07 mV ($n = 184$ neurons). PAG neurons depolarized rapidly in response to LPI, and the membrane potential returned slowly to baseline (Fig. 5A). The response was concentration dependent—0.1, 1, and 10 μM LPI depolarized PAG neurons by 0.41 ± 0.23 mV ($n = 48$), 3.14 ± 0.46 mV ($n = 43$), and 8.72 ± 0.61 mV ($n = 39$), respectively; statistical significance was achieved for the latter two concentrations of LPI ($P < 0.00001$; Fig. 5B). The effect to LPI (10 μM) was abolished in neurons pretreated with the GPR55 antagonist ML-193 (10 μM, 20 minutes;

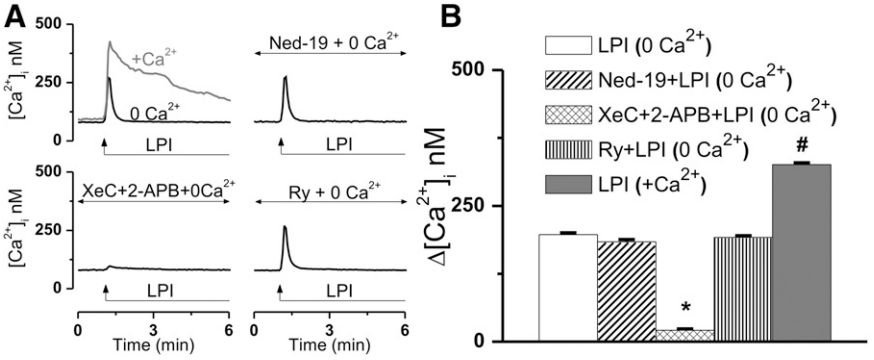

Fig. 3. LPI mobilizes inositol 1,4,5-trisphoshate–sensitive Ca^{2+} stores. (A) Characteristic examples of Ca^{2+} responses triggered by LPI (10 μM) administration in PAG neurons incubated with Ca^{2+}-free saline in the absence or presence of two pore channel blocker Ned-19, IP_3R blockers xestospongin C (XeC), and 2-aminoethoxydiphenyl borate (2-APB) or ryanodine receptor blocker ryanodine (Ry); the effect of LPI administration in Ca^{2+}-containing saline is depicted by the gray trace in the first panel (included for comparison purposes). (B) Comparison of the Ca^{2+} responses produced by the indicated treatments; $P < 0.00001$ compared with LPI alone in Ca^{2+} free saline (*) or to all other treatments (#).

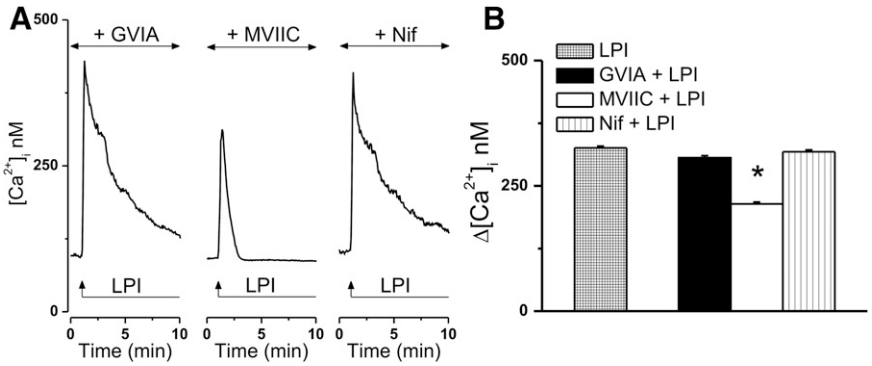

Fig. 4. LPI activates voltage-gated P/Q channels. (A) Representative increases in $[Ca^{2+}]_i$ elicited by LPI (10 μM) in PAG neurons pretreated with blockers of N-type (ω-conotoxin GVIA), P/Q-type (ω-conotoxin MVIIC), and L-type (nifedipine, Nif) of voltage-gated Ca^{2+} channels. (B) Comparison of the Ca^{2+} responses produced by the indicated treatments; $^*P < 0.00001$ compared with LPI alone.

ΔVm = 1.8 ± 0.34 mV, n = 54; Fig. 5, A and B). The effects of LPI on cultured neurons were confirmed by electrophysiological recordings of neurons located in the lateral and ventrolateral PAG in midbrain slices. Figure 6A shows a representative recording of a PAG neuron that depolarized in response to 10 μM LPI from a baseline of –54.8 to –45.8 mV, with minimal changes in input resistance. The amplitude of the depolarization was similar to that observed in cell cultures and sufficient to trigger action potential firing (Fig. 6A). LPI (10 or 20 μM) depolarized 11 neurons from –53.7 ± 2.6 to –42.1 ± 2.4 mV ($P <$ 0.01, paired t test; Fig. 6B). Seven cells received 10 μM LPI and 4 cells 20 μM LPI; unpaired t test showed no significant differences for baseline Vm or input resistance or LPI response for either Vm or input resistance. The input resistance was largely similar before (362 ± 44 MΩ) and after LPI application (393 ± 50 MΩ, n = 11, P = 0.29; Fig. 6C).

GPR55 Ligands Modulate Nociception in the PAG. We examined the effects of intra-PAG administration of LPI on animal paw withdrawal or paw licking latency in the hot-plate test. After the injection of LPI (1 μg/0.5 μl), the hot-plate latency was reduced significantly with a maximum effect of 5.72 ± 0.52 seconds in comparison with control (11.36 ± 1.06 seconds) ($P < 0.001$; Fig. 7). Pretreatment with ML-193 (1 μg/0.5 μl, 15 minutes before LPI), antagonized the LPI-induced nociception (Fig. 7). ML-193 at a dose of 1 μg/0.5 μl by itself induced an increase in hot-plate latency compared with control group (vehicle/vehicle), with a maximum effect of 14.97 ± 1.455 at 30–45 minutes postinjection [$P < 0.001$, two-way analysis of variance with repeated measures (latency × time), followed by Bonferroni posttest; Fig. 7], indicating that ML-193 is antinociceptive. Mean responses before injection were as follows: 10.29 ± 0.5 seconds (LPI + vehicle); 10.78 ± 0.2 seconds (ML-193 + vehicle); 10.67 ± 0.20 seconds (ML-193 + LPI), and 10.84 ± 0.20 seconds (vehicle + vehicle). Groups consisted of 4 to 6 animals.

Discussion

The present study identifies GPR55 as an important player modulating descending pain pathways in the PAG. As shown here, cultured PAG neurons respond to LPI application by increasing their $[Ca^{2+}]_i$ and depolarizing neuronal membrane in a concentration- and GPR55-dependent manner, effects further translated in vivo into centrally mediated pronociceptive behavioral responses.

We and others previously reported that LPI-induced activation of GPR55 is associated with Ca^{2+} signaling in neurons and other cell types (Lauckner et al., 2008; Pineiro and Falasca, 2012; Yu et al., 2013).

Ca^{2+} responses in PAG neurons may differentially impact modulatory pain signals originating in this brain region. For instance, opioids inhibit voltage-gated Ca^{2+} conductances in dissociated PAG neurons (Connor and Christie, 1998), whereas cannabinoids have no effect on postsynaptic Ca^{2+} currents in the PAG (Vaughan et al., 2000). Nonetheless, both opioids and cannabinoids promote descending analgesia in the PAG via a disinhibitory mechanism involving inhibition of GABAergic interneurons synapsing onto non-GABAergic PAG-rostral ventrolateral medulla projection neurons (Basbaum and Fields, 1984; Vaughan and Christie, 1997; Vaughan et al., 2000). On a different note, opioid analgesia has been associated with T-type Ca^{2+} channel activation in low threshold-spiking μ opioid receptor–positive GABAergic neurons in the ventrolateral PAG, resulting in neuronal inhibition (Park et al., 2010).

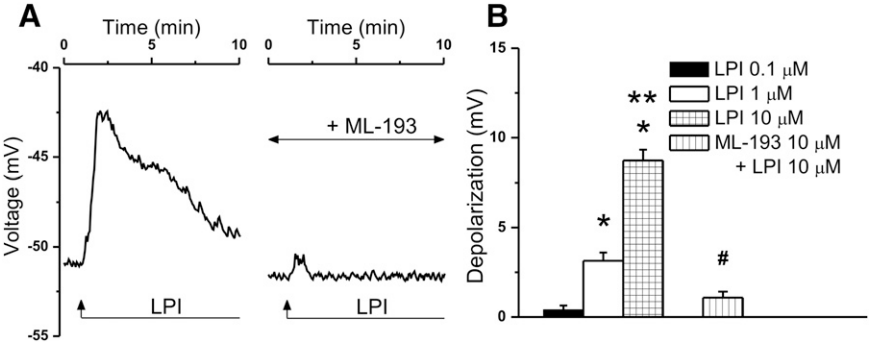

Fig. 5. LPI depolarizes cultured PAG neurons via GPR55. (A) Characteristic recordings of membrane potential changes induced by LPI (10 μM) administration in naive PAG neurons and in PAG neurons pretreated with ML-193 (10 μM). (B) Concentration-dependent depolarizing effect of LPI (0.1, 1, and 10 μM) and lack of effect of LPI (10 μM) in neurons treated with ML-193 (10 μM); $P < 0.00001$ compared with basal (*), to any other concentration of LPI (**), or to 10 μM LPI (#).

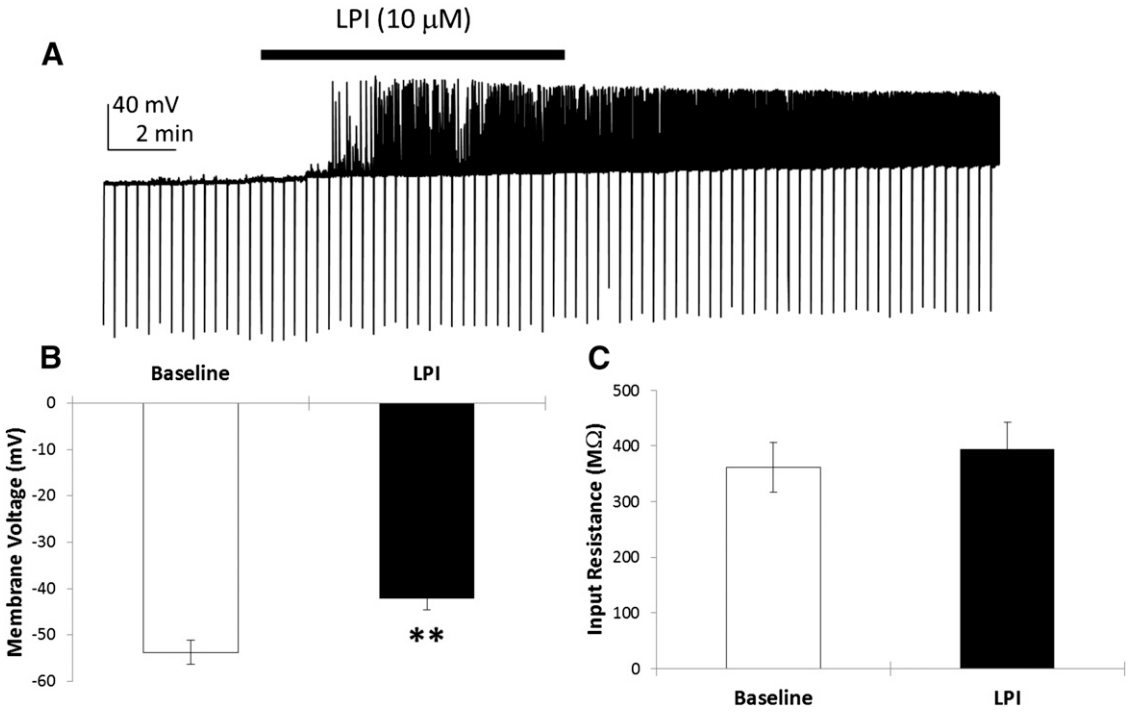

Fig. 6. LPI depolarizes PAG neurons in acute midbrain slices. (A) Characteristic continuous current-clamp recording of a ventrolateral PAG neuron in which LPI (10 μM) application produced a depolarization associated with action potential firing. (B) LPI depolarized neurons with a mean value of 11.6 $\pm$ 3.2 mV (n = 11; $^{**}P < 0.01$, paired t test). (C) The input resistance is not significantly modified by LPI treatment (P = 0.29).

We show here that in dissociated PAG neurons, LPI induces a rapid and sharp Ca^{2+} response, followed by a slow return to baseline. The initial fast peak in $[Ca^{2+}]_i$ appears to be mediated both by endoplasmic reticulum Ca^{2+} release via IP_3Rs and by Ca^{2+} entry via P/Q-type of VGCC, whereas only the latter mechanism is responsible for the slow recovery phase. Interestingly, P/Q-type Ca^{2+} channel blockade in the PAG facilitates trigeminal nociception (Knight et al., 2002), while having no effect on bicuculline-induced analgesia in a similar animal model of pain (Knight et al., 2003). Conversely, nociceptin, which promotes analgesia in the PAG via both pre- and postsynaptic mechanisms (Vaughan et al., 1997), has been found to inhibit P/Q-type Ca^{2+} channels in PAG neurons (Connor and Christie, 1998). We propose that the particular Ca^{2+} pathway coupled to GPR55 activation in the PAG is responsible for its pronociceptive effect. This is not unusual because Ca^{2+} release from distinct stores has critical functional implications and the shape and amplitude of the Ca^{2+} signals also modulate distinct cellular functions (Rizzuto and Pozzan, 2006). Moreover, we previously reported that GPR55 stimulation can result in activation of distinct signaling cascades involving Ca^{2+} as a second messenger, which differentially impact membrane polarization (Yu et al., 2013).

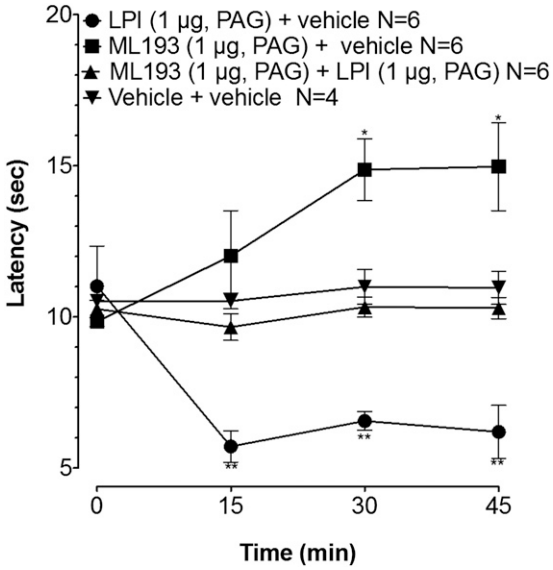

Fig. 7. Time course of GPR55-mediated effects on nociception in the hot-plate test. LPI (1 μg/0.5 μl) or an equivalent volume of vehicle was microinjected at time zero. ML-193 (1 μg/0.5 μl) was given 15 minutes before LPI. The nociceptive response is expressed as the mean $\pm$ S.E.M. in seconds (sec). N, number of rats. Mean response before injection was as follows: ● = 10.29 $\pm$ 0.5 seconds; ■ = 10.78 $\pm$ 0.2 seconds; ▲ = 10.67 $\pm$ 0.20 seconds; and ▼=10. 84 $\pm$ 0.20 seconds. $P < 0.05$ (*) and $P < 0.01$ (**) compared with the corresponding time point of the vehicle + vehicle group (▼) or to ML193 + LPI group (▲).

In the case of cultured PAG neurons, we find that GPR55 activation is associated with neuronal membrane depolarization. Similarly, LPI depolarized neurons located in the lateral and ventrolateral PAG in midbrain slices. This response is further translated in vivo in a reduction of the nociceptive threshold in the hot-plate test, at 52°C, in response to LPI microinjection into the PAG. Although we observed a pronociceptive effect of GPR55 activation in male rats, it is interesting that studies using global deletion of GPR55 indicate an impact on nociception in the hot-plate test in only female animals (Staton et al., 2008; Wu et al., 2013). Because the hot-plate test evaluates pain as a result of supraspinal sensory integration (Caggiula et al., 1995; Rubinstein et al., 1996), a putative explanation may reside in the fact that

GPR55 is expressed at pain-relevant supraspinal sites other than the PAG (Henstridge et al., 2011), where the effects of its activation may interfere with sexual hormone-mediated signaling.

We note that the significant effects of LPI observed in this study occurred at concentrations of 1 and 10 μM, which are well in the range of tissue concentrations that can be reached in pathophysiological states in vivo (Shen et al., 2001; Xiao et al., 2001; Sutphen et al., 2004; Ross, 2011) and largely similar to those promoting cellular effects in vitro (Falasca et al., 1995; Lauckner et al., 2008; Yu et al., 2013). Brain concentration of lipids, and implicitly, LPI, are difficult to evaluate due to limitations in extraction procedures, specificity, and rapid degradation. Thus, extracellular levels of LPI in the PAG are difficult to estimate. However, there may be a significant level of endogenous activation of GPR55 in the PAG, promoting descending pain facilitation, because microinjection of ML-193 alone resulted in an analgesic effect in vivo.

LPI levels are increased in the caudal medulla oblongata of carrageenan-injected rats (Ma et al., 2012). Moreover, LPI is intracellularly generated by cPLA2 (Pineiro and Falasca, 2012), and central cPLA2 inhibition diminishes pain perception in mice undergoing facial carrageenan injection (Yeo et al., 2004). These findings support the notion that pain-generating conditions associate with central LPI accumulation and that LPI is a nociceptive mediator in the descending pathways. The present study identifies GPR55 as a novel messenger of LPI-induced descending pain facilitation.

Together, our data represent the first pharmacological evidence of GPR55 involvement in central pain processing and unravel a novel Ca^{2+}-mediated mechanism by which PAG neurons are activated downstream of GPR55. Moreover, the identification of GPR55 as a pronociceptive modulator in the PAG provides an explanation for the absence of hyperalgesia in GPR55(−/−) animals in inflammatory and neuropathic pain models (Staton et al., 2008) and further supports interference with GPR55 activation in the PAG to promote analgesia.

Authorship Contributions:

Participated in research design: Deliu, Sperow, Console-Bram, Kalamarides, Kirby, G. C. Brailoiu, E. Brailoiu, Benamar, Abood.

Conducted experiments: Deliu, Sperow, Console-Bram, Carter, Kalamarides, G. C. Brailoiu, E. Brailoiu.

Contributed new reagents or analytic tools: Tilley, Abood.

Performed data analysis: Deliu, Sperow, Console-Bram, Kalamarides, Kirby, G. C. Brailoiu, E. Brailoiu, Benamar.

Wrote or contributed to the writing of the manuscript: Deliu, Sperow, Console-Bram, Kalamarides, G. C. Brailoiu, E. Brailoiu, Benamar, Abood.

References

Basbaum AI and Fields HL (1984) Endogenous pain control systems: brainstem spinal pathways and endorphin circuitry. *Annu Rev Neurosci* **7**:309–338.

Benamar K, Geller EB, and Adler MW (2008a) First in vivo evidence for a functional interaction between chemokine and cannabinoid systems in the brain. *J Pharmacol Exp Ther* **325**:641–645.

Benamar K, Geller EB, and Adler MW (2008b) A new brain area affected by 3,4-methylenedioxymethamphetamine: A microdialysis-biotelemetry study. *Eur J Pharmacol* **596**:84–88.

Bilmen JG and Michelangeli F (2002) Inhibition of the type 1 inositol 1,4,5-trisphosphate receptor by 2-aminoethoxydiphenylborate. *Cell Signal* **14**:955–960.

Brailoiu GC, Deliu E, Hooper R, Dun NJ, Undieh AS, Adler MW, Benamar K, and Brailoiu E (2012) Agonist-selective effects of opioid receptor ligands on cytosolic calcium concentration in rat striatal neurons. *Drug Alcohol Depend* **123**:277–281.

Caggiula AR, Epstein LH, Perkins KA, and Saylor S (1995) Different methods of assessing nicotine-induced antinociception may engage different neural mechanisms. *Psychopharmacology (Berl)* **122**:301–306.

Chen X, Kirby LG, Palma J, Benamar K, Geller EB, Eisenstein TK, and Adler MW (2011) The effect of gp120 on morphine's antinociceptive and neurophysiological actions. *Brain Behav Immun* **25**:1434–1443.

Connor M and Christie MJ (1998) Modulation of Ca2+ channel currents of acutely dissociated rat periaqueductal grey neurons. *J Physiol* **509**:47–58.

Deliu E, Brailoiu GC, Arterburn JB, Oprea TI, Benamar K, Dun NJ, and Brailoiu E (2012) Mechanisms of G protein-coupled estrogen receptor-mediated spinal nociception. *J Pain* **13**:742–754.

Deliu E, Brailoiu GC, Eguchi S, Hoffman NE, Rabinowitz JE, Tilley DG, Madesh M, Koch WJ, and Brailoiu E (2014) Direct evidence of intracrine angiotensin II signaling in neurons. *Am J Physiol Cell Physiol* **306**:C736–C744.

Falasca M, Silletta MG, Carvelli A, Di Francesco AL, Fusco A, Ramakrishna V, and Corda D (1995) Signalling pathways involved in the mitogenic action of lysophosphatidylinositol. *Oncogene* **10**:2113–2124.

Gafni J, Munsch JA, Lam TH, Catlin MC, Costa LG, Molinski TF, and Pessah IN (1997) Xestospongins: potent membrane permeable blockers of the inositol 1,4,5-trisphosphate receptor. *Neuron* **19**:723–733.

Gangadharan V, Selvaraj D, Kurejova M, Njoo C, Gritsch S, Škoricová D, Horstmann H, Offermanns S, Brown AJ, and Kuner T et al. (2013) A novel biological role for the phospholipid lysophosphatidylinositol in nociceptive sensitization via activation of diverse G-protein signalling pathways in sensory nerves in vivo. *Pain* **154**: 2801–2812.

Heinisch S and Kirby LG (2010) SDF-1alpha/CXCL12 enhances GABA and glutamate synaptic activity at serotonin neurons in the rat dorsal raphe nucleus. *Neuropharmacology* **58**:501–514.

Heinricher MM, Tavares I, Leith JL, and Lumb BM (2009) Descending control of nociception: Specificity, recruitment and plasticity. *Brain Res Brain Res Rev* **60**: 214–225.

Henstridge CM (2012) Off-target cannabinoid effects mediated by GPR55. *Pharmacology* **89**:179–187.

Henstridge CM, Balenga NA, Kargl J, Andradas C, Brown AJ, Irving A, Sanchez C, and Waldhoer M (2011) Minireview: recent developments in the physiology and pathology of the lysophosphatidylinositol-sensitive receptor GPR55. *Mol Endocrinol* **25**:1835–1848.

Heynen-Genel S, Dahl R, Shi S, Milan L, Hariharan S, Sergienko E, Hedrick M, Dad S, Stonich D, Su Y, et al. (2010) Screening for selective ligands for GPR55 - Antagonists. Probe Reports from the NIH Molecular Libraries Program. National Center for Biotechnology Information, Bethesda, MD; 2010 Oct 30 [updated 2011 May 26].

Kapur A, Zhao P, Sharir H, Bai Y, Caron MG, Barak LS, and Abood ME (2009) Atypical responsiveness of the orphan receptor GPR55 to cannabinoid ligands. *J Biol Chem* **284**:29817–29827.

Knight YE, Bartsch T, and Goadsby PJ (2003) Trigeminal antinociception induced by bicuculline in the periaqueductal gray (PAG) is not affected by PAG P/Q-type calcium channel blockade in rat. *Neurosci Lett* **336**:113–116.

Knight YE, Bartsch T, Kaube H, and Goadsby PJ (2002) P/Q-type calcium-channel blockade in the periaqueductal gray facilitates trigeminal nociception: a functional genetic link for migraine? *J Neurosci* **22**:1–6.

Lauckner JE, Jensen JB, Chen HY, Lu HC, Hille B, and Mackie K (2008) GPR55 is a cannabinoid receptor that increases intracellular calcium and inhibits M current. *Proc Natl Acad Sci USA* **105**:2699–2704.

Ma MT, Yeo JF, Shui G, Wenk MR, and Ong WY (2012) Systems wide analyses of lipids in the brainstem during inflammatory orofacial pain - evidence of increased phospholipase A(2) activity. *Eur J Pain* **16**:38–48.

Maruyama T, Kanaji T, Nakade S, Kanno T, and Mikoshiba K (1997) 2APB, 2-aminoethoxydiphenyl borate, a membrane-penetrable modulator of Ins(1,4,5)P3-induced Ca2+ release. *J Biochem* **122**:498–505.

Naylor E, Arredouani A, Vasudevan SR, Lewis AM, Parkesh R, Mizote A, Rosen D, Thomas JM, Izumi M, and Ganesan A et al. (2009) Identification of a chemical probe for NAADP by virtual screening. *Nat Chem Biol* **5**:220–226.

Park C, Kim JH, Yoon BE, Choi EJ, Lee CJ, and Shin HS (2010) T-type channels control the opioidergic descending analgesia at the low threshold-spiking GABAergic neurons in the periaqueductal gray. *Proc Natl Acad Sci USA* **107**: 14857–14862.

Paxinos G and Watson C (1988) *The rat brain in stereotaxic coordinates*, Academic Press, San Diego.

Piñeiro R and Falasca M (2012) Lysophosphatidylinositol signalling: new wine from an old bottle. *Biochim Biophys Acta* **1821**:694–705.

Porreca F, Ossipov MH, and Gebhart GF (2002) Chronic pain and medullary descending facilitation. *Trends Neurosci* **25**:319–325.

Rizzuto R and Pozzan T (2006) Microdomains of intracellular Ca2+: molecular determinants and functional consequences. *Physiol Rev* **86**:369–408.

Ross RA (2011) L-α-lysophosphatidylinositol meets GPR55: a deadly relationship. *Trends Pharmacol Sci* **32**:265–269.

Rubinstein M, Mogil JS, Japón M, Chan EC, Allen RG, and Low MJ (1996) Absence of opioid stress-induced analgesia in mice lacking beta-endorphin by site-directed mutagenesis. *Proc Natl Acad Sci USA* **93**:3995–4000.

Shen Z, Wu M, Elson P, Kennedy AW, Belinson J, Casey G, and Xu Y (2001) Fatty acid composition of lysophosphatidic acid and lysophosphatidylinositol in plasma from patients with ovarian cancer and other gynecological diseases. *Gynecol Oncol* **83**:25–30.

Staton PC, Hatcher JP, Walker DJ, Morrison AD, Shapland EM, Hughes JP, Chong E, Mander PK, Green PJ, and Billinton A et al. (2008) The putative cannabinoid receptor GPR55 plays a role in mechanical hyperalgesia associated with inflammatory and neuropathic pain. *Pain* **139**:225–236.

Sutphen R, Xu Y, Wilbanks GD, Fiorica J, Grendys EC, Jr, LaPolla JP, Arango H, Hoffman MS, Martino M, and Wakeley K et al. (2004) Lysophospholipids are potential biomarkers of ovarian cancer. *Cancer Epidemiol Biomarkers Prev* **13**: 1185–1191.

Vaughan CW and Christie MJ (1997) Presynaptic inhibitory action of opioids on synaptic transmission in the rat periaqueductal grey in vitro. *J Physiol* **498**: 463–472.

Vaughan CW, Connor M, Bagley EE, and Christie MJ (2000) Actions of cannabinoids on membrane properties and synaptic transmission in rat periaqueductal gray neurons in vitro. *Mol Pharmacol* **57**:288–295.
Vaughan CW, Ingram SL, and Christie MJ (1997) Actions of the ORL1 receptor ligand nociceptin on membrane properties of rat periaqueductal gray neurons in vitro. *J Neurosci* **17**:996–1003.
Wu CS, Chen H, Sun H, Zhu J, Jew CP, Wager-Miller J, Straiker A, Spencer C, Bradshaw H, and Mackie K et al. (2013) GPR55, a G-protein coupled receptor for lysophosphatidylinositol, plays a role in motor coordination. *PLoS ONE* **8**:e60314.
Xiao YJ, Schwartz B, Washington M, Kennedy A, Webster K, Belinson J, and Xu Y (2001) Electrospray ionization mass spectrometry analysis of lysophospholipids in human ascitic fluids: comparison of the lysophospholipid contents in malignant vs nonmalignant ascitic fluids. *Anal Biochem* **290**:302–313.
Yeo JF, Ong WY, Ling SF, and Farooqui AA (2004) Intracerebroventricular injection of phospholipases A2 inhibitors modulates allodynia after facial carrageenan injection in mice. *Pain* **112**:148–155.
Yu J, Deliu E, Zhang XQ, Hoffman NE, Carter RL, Grisanti LA, Brailoiu GC, Madesh M, Cheung JY, and Force T et al. (2013) Differential activation of cultured neonatal cardiomyocytes by plasmalemmal versus intracellular G protein-coupled receptor 55. *J Biol Chem* **288**:22481–22492.

Address correspondence to: Mary E. Abood, Center for Substance Abuse Research, Temple University School of Medicine, 3500 N. Broad Street, Room 852, Philadelphia, PA 19140. E-mail: mabood@temple.edu